The 8th European Congress on Computational Methods in Applied Sciences and Engineering
ECCOMAS Congress 2022
5-–9 June 2022, Oslo, Norway

EXTENDED VIRTUAL ELEMENT METHOD FOR FRACTURE MODELING IN TWO-DIMENSIONAL LINEAR ELASTICITY

ANDREA CHIOZZI[1], ELENA BENVENUTI[2], GIANMARCO MANZINI[3] AND N. SUKUMAR[4]

[1] Department of Environmental and Prevention Sciences
University of Ferrara
Via Saragat 1, 44122 Ferrara, Italy
e-mail: andrea.chiozzi@unife.it

[2] Department of Engineering
University of Ferrara
Via Saragat 1, 44122 Ferrara, Italy
e-mail: bnvlne@unife.it

[3] Istituto di Matematica Applicata e Tecnologie Informatiche
Consiglio Nazionale delle Ricerche
Via A. Ferrata 5, 27100 Pavia, Italy
e-mail: marco.manzini@imati.cnr.it

[4] Department of Civil and Environmental Engineering
University of California, Davis
One Shields Avenue, 95616 Davis, CA, USA
e-mail: nsukumar@ucdavis.edu

Key words: virtual element method, extended finite element method, fracture, singularities

Abstract. The virtual element method (VEM), is a stabilized Galerkin scheme deriving from mimetic finite differences, which allows for very general polygonal meshes, and does not require the explicit knowledge of the shape functions within the problem domain. In the VEM, the discrete counterpart of the continuum formulation of the problem is defined by means of a suitable projection of the virtual shape functions onto a polynomial space, which allows the decomposition of the bilinear form into a consistent part, reproducing the polynomial space, and a correction term ensuring stability. In the present contribution, we outline an extended virtual element method (X-VEM) for two-dimensional elastic fracture problems where, drawing inspiration from the extended finite element method (X-FEM), we extend the standard virtual element space with the product of vector-valued virtual nodal shape functions and suitable enrichment fields, which reproduce the singularities of the exact solution. We define an extended projection operator that maps functions in the extended virtual element space onto a set spanned by the space of linear polynomials augmented with the enrichment fields. Numerical examples in 2D elastic fracture are worked out to assess convergence and accuracy of the proposed method for both quadrilateral and general polygonal meshes.

1 INTRODUCTION

Numerical techniques for the solution of problems that admit singular or discontinuous solutions such as fracture propagation in solids have attracted significant attention in the last two decades. In particular, to date, enriched finite element approximations based on the partition-of-unity concept [1, 2] and the eXtended Finite Element Method (X-FEM) [3] have proven to be one of the most successful methods to analyse fracture problems on unstructured meshes without requiring remeshing. More recently, extended finite element formulations for polygonal meshes have been proposed [4, 5]. However, on polygonal elements, the construction of shape functions is generally cumbersome and, when dealing with singular functions, additional numerical integration issues must be carefully dealt with [6, 7, 8].

The Virtual Element Method (VEM) is a stabilized Galerkin scheme proposed in [9] to solve partial differential equations on general polygonal meshes that overcomes many of the difficulties related to standard polygonal finite element formulations. The VEM can be looked at as a generalization of the Finite Element Method (FEM) in which the explicit knowledge of the basis functions is not needed. Indeed, in the VEM, the bilinear form and the continuous linear functional deriving from the variational formulation, are approximated by means of elliptic projections of the basis functions onto suitable polynomial spaces, which turn out to be computable from the degrees of freedom of the method. The VEM has also been proposed for the solution of two- and three-dimensional linear elasticity [10, 11] and several studies have exploited the flexibility of the method to deal with meshes that are cut by discontinuities in fracture problems [12, 13, 14]. More recently, taking inspiration from the X-FEM, an eXtended Virtual Element Method (X-VEM) has been proposed in [15, 16], for the scalar Laplace problem with singularities and discontinuities, and in [17] for fracture problems in two-dimensional linear elasticity.

In this contribution, we summarize the main finding related to the extended virtual element formulation for linear elastic fracture problems proposed in [17], in which the displacement field features both discontinuities and crack-tip singularities. The method entails the construction of an enriched virtual element space by means of an additional set of virtual basis functions built on suitably chosen vectorial enrichment fields which allow to incorporate additional information about the exact solution, taming the negative effects of the singularity on numerical accuracy. On the other hand, discontinuities in the displacement field are embedded into the virtual element space using the approach proposed for finite elements by Hansbo and Hansbo [18]. The X-VEM for elastic fracture provides greater flexibility with respect to the X-FEM since it is applicable to arbitrary polygonal meshes and, unlike the X-FEM where numerical integration generally leads to several issues, a one-dimensional quadrature rule on the boundary of the polygonal element suffices to compute weak form integrals.

2 TWO-DIMENSIONAL ELASTICITY MODEL

Let us consider a linear elastic body occupying the two-dimensional domain $\Omega \subset \mathbb{R}^2$, bounded by Γ e cut by a traction-free internal crack Γ_c. We denote the displacement field on Ω by $\boldsymbol{u}(\boldsymbol{x})$ and assume small strains and displacements. The boundary $\Gamma = \Gamma_u \cup \Gamma_t \cup \Gamma_c$, where Γ_u, Γ_t and Γ_c are nonoverlapping. Prescribed displacements $\boldsymbol{g} \in C^0(\Gamma_u)$ are imposed on Γ_u, whereas tractions $\bar{\boldsymbol{t}} \in C^0(\Gamma_t)$ are imposed on Γ_t.

Let $\boldsymbol{\sigma}$ be the Cauchy stress tensor. In the absence of body forces, equilibrium equations read

$$\nabla \cdot \boldsymbol{\sigma} = \mathbf{0} \qquad \text{in } \Omega, \tag{1a}$$

with the natural boundary conditions

$$\boldsymbol{\sigma} \cdot \boldsymbol{n} = \bar{\boldsymbol{t}} \qquad \text{on } \Gamma_t, \tag{1b}$$
$$\boldsymbol{\sigma} \cdot \boldsymbol{n} = \mathbf{0} \qquad \text{on } \Gamma_c, \tag{1c}$$

where $\boldsymbol{n}$ is the unit outward normal, and the essential boundary condition

$$\boldsymbol{u} = \boldsymbol{g} \qquad \text{on } \Gamma_u. \tag{1d}$$

The small strain tensor $\boldsymbol{\varepsilon}$ is related to the displacement field $\boldsymbol{u}$ by the compatibility equation

$$\boldsymbol{\varepsilon}(\boldsymbol{u}) = \frac{1}{2}\left(\nabla(\boldsymbol{u}) + \nabla^T(\boldsymbol{u})\right), \tag{1e}$$

Lastly, the isotropic linear elastic constitutive for a homogeneous material reads

$$\boldsymbol{\sigma}(\boldsymbol{u}) = \boldsymbol{C} : \boldsymbol{\varepsilon}(\boldsymbol{u}), \tag{1f}$$

where $\boldsymbol{C}$ is the fourth-order elasticity tensor.

To state the weak form of the problem we define the space of admissible displacement fields as

$$\mathscr{U} = \left\{\boldsymbol{v} \in [H^1(\Omega)]^2 : \boldsymbol{v} = \boldsymbol{g} \text{ on } \Gamma_u,\ \boldsymbol{v} \text{ discontinuous on } \Gamma_c\right\}, \tag{2}$$

Similarly, the test function space is defined as:

$$\mathscr{U}_0 = \left\{\boldsymbol{v} \in [H^1(\Omega)]^2 : \boldsymbol{v} = 0 \text{ on } \Gamma_u,\ \boldsymbol{v} \text{ discontinuous on } \Gamma_c\right\}. \tag{3}$$

The weak form of the equilibrium equation reads as: Find $\boldsymbol{u} \in \mathscr{U}$ such that

$$a(\boldsymbol{u}, \boldsymbol{v}) := \int_\Omega \boldsymbol{\sigma}(\boldsymbol{v}) : \boldsymbol{\varepsilon}(\boldsymbol{u})\, d\boldsymbol{x} = \int_{\Gamma_t} \bar{\boldsymbol{t}} \cdot \boldsymbol{v} d\Gamma =: b(\boldsymbol{v}) \quad \forall \boldsymbol{v} \in \mathscr{U}_0. \tag{4}$$

3 EXTENDED VIRTUAL ELEMENT FORMULATION

We now summarize the formulation of the extended virtual element method for fracture problems in two-dimensional elasticity presented in [17]. Let $\mathcal{T} = \{\Omega_h\}_h$ be a family of decompositions of Ω into nonoverlapping polygonal elements E with nonintersecting boundary ∂E, barycenter $\boldsymbol{x}_E \equiv (x_E, y_E)^T$, area $|E|$, and diameter $h_E = \sup_{\boldsymbol{x},\boldsymbol{y}\in E} |\boldsymbol{x} - \boldsymbol{y}|$.

3.1 Enrichment with singular fields

The main concept of the X-VEM is to enrich the standard virtual element space by means of independent fields carrying information about the singularities affecting the exact solution. For the problem at hand, we choose the enrichment fields $\check{\boldsymbol{u}}^I = \boldsymbol{u}^I/h^{1/2}$ and $\check{\boldsymbol{u}}^{II} = \boldsymbol{u}^{II}/h^{1/2}$, where $\boldsymbol{u}^I$ and $\boldsymbol{u}^{II}$ are the exact asymptotic crack-tip displacement fields for mode I and mode II crack opening respectively, and h the maximum elemental diameter of the mesh [17]. We observe that these fields satisfy equilibrium. In order to define the extended virtual element space, we first introduce the local virtual element space $\boldsymbol{V}^{h,*}(E)$:

$$\boldsymbol{V}^{h,*}(E) \equiv \left\{ \boldsymbol{v}^h = (v_x^h, v_y^h)^T \in \boldsymbol{V}^h(E) : v_x^h = v_y^h \right\}, \tag{5}$$

where $\boldsymbol{V}^h(E) = [V^h(E)]^2$ with $V^h(E)$ the standard virtual element space, spanned by the scalar virtual basis functions $\{\varphi_i\}_{i=1}^{N_E}$. Hence, the space $\boldsymbol{V}^{h,*}(E)$ is generated by the linear combination of the basis functions $\{\boldsymbol{\varphi}_i^* = (\varphi_i, \varphi_i)^T\}_{i=1}^{N_E}$. Then, we define the matrices $\boldsymbol{\psi}^I$ and $\boldsymbol{\psi}^{II}$ as

$$\boldsymbol{\psi}^I \equiv \begin{bmatrix} \check{u}_x^I & 0 \\ 0 & \check{u}_y^I \end{bmatrix}, \quad \boldsymbol{\psi}^{II} \equiv \begin{bmatrix} \check{u}_x^{II} & 0 \\ 0 & \check{u}_y^{II} \end{bmatrix}, \tag{6}$$

so that the *local extended virtual element space* $\boldsymbol{V}_X^h(E)$ reads as

$$\boldsymbol{V}_X^h(E) \equiv \boldsymbol{V}^h(E) \oplus \boldsymbol{\psi}^I \boldsymbol{V}^{h,*}(E) \oplus \boldsymbol{\psi}^{II} \boldsymbol{V}^{h,*}(E). \tag{7}$$

A basis of this space can be obtained as the union of the basis functions of $\boldsymbol{V}_X^h(E)$, $\boldsymbol{\psi}^I \boldsymbol{V}^{h,*}(E)$ and $\boldsymbol{\psi}^{II} \boldsymbol{V}^{h,*}(E)$. Therefore, at every enriched node the vector-valued field $\boldsymbol{v}_X^h(\boldsymbol{x})$ that belongs to the extended virtual element space $\boldsymbol{V}_X^h(E)$ is characterized by four values and for an element whose nodes are all enriched, we have $4N_E$ degrees of freedom. We denote the basis functions of $\boldsymbol{V}_X^h(E)$ by the symbol $\boldsymbol{\varphi}_i$, $i = 1, 2, \ldots, 4N_E$, where

$$\boldsymbol{\varphi}_i = \begin{cases} \Big(\varphi_i, 0\Big)^T & \text{for } 1 \le i \le 2N_E, \ i \text{ odd}, \\ \Big(0, \varphi_i\Big)^T & \text{for } 1 \le i \le 2N_E, \ i \text{ even}, \\ \Big(\check{u}_x^I \varphi_i, \check{u}_y^I \varphi_i\Big)^T & \text{for } 1 + 2N_E \le i \le 3N_E, \\ \Big(\check{u}_x^{II} \varphi_i, \check{u}_y^{II} \varphi_i\Big)^T & \text{for } 1 + 3N_E \le i \le 4N_E. \end{cases}$$

Finally, the extended global virtual element space $\boldsymbol{V}_X^h$ reads:

$$\boldsymbol{V}_X^h = \Big\{ \boldsymbol{v}_X^h \in \big[H^1(\Omega)\big]^2 : \boldsymbol{v}_{X|E}^h \in \boldsymbol{V}_X^h(E) \quad \forall E \in \Omega_h \Big\}.$$

Since $\{\boldsymbol{\varphi}_i\}_{i=1}^{4N_E}$ are not known in the interior of the element, we construct a convenient projection operator that allows to compute the approximations $a_X^h(\cdot,\cdot) : \boldsymbol{V}_X^h(E) \times \boldsymbol{V}_X^h(E) \to \mathbb{R}$ and $b_X^h(\cdot) : \boldsymbol{V}_X^h(E) \to \mathbb{R}$ of the exact bilinear form $a(\cdot,\cdot)$ and the linear functional $b(\cdot)$ appearing in (4). The extended virtual element formulation then reads: Find $\boldsymbol{u}_X^h \in \boldsymbol{V}_{X,\boldsymbol{g}}^h$ such that

$$a_X^h(\boldsymbol{u}_X^h, \boldsymbol{v}_X^h) = b_X^h(\boldsymbol{v}_X^h) \quad \forall \boldsymbol{v}_X^h \in \boldsymbol{V}_{X,\boldsymbol{0}}^h, \tag{8}$$

where the bilinear form $a_X^h(\cdot,\cdot)$ is built element-wise as

$$a_X^h(\boldsymbol{u}_X^h, \boldsymbol{v}_X^h) = \sum_{E\in\Omega} a_X^{h,E}(\boldsymbol{u}_X^h, \boldsymbol{v}_X^h) \quad \forall \boldsymbol{u}_X^h, \boldsymbol{v}_X^h \in \boldsymbol{V}_X^h, \tag{9}$$

and we set $b_X^h(\boldsymbol{v}_X^h) = b(\boldsymbol{v}_X^h)$. To construct a bilinear form $a_X^{h,E}(\cdot,\cdot)$ which is computable from the degrees of freedom, we extend the vector-valued linear polynomial space $\mathbb{P}^1(E)$ to a subspace $\mathbb{P}_X$ of $\boldsymbol{V}_X^h(E)$ which includes the linear polynomials and the additional enrichment functions $\check{\boldsymbol{u}}^I$ and $\check{\boldsymbol{u}}^{II}$. Such space is spanned by the eight linearly independent vector fields representing the three fundamental rigid body motions, the three independent deformation modes and the two enrichment fields:

$$\mathbb{P}_X(E) = \text{span}\left\{ \begin{pmatrix} 1 \\ 0 \end{pmatrix}, \begin{pmatrix} 0 \\ 1 \end{pmatrix}, \begin{pmatrix} \eta \\ -\xi \end{pmatrix}, \begin{pmatrix} \xi \\ 0 \end{pmatrix}, \begin{pmatrix} 0 \\ \eta \end{pmatrix}, \begin{pmatrix} \eta \\ \xi \end{pmatrix}, \begin{pmatrix} \check{u}_x^I \\ \check{u}_y^I \end{pmatrix}, \begin{pmatrix} \check{u}_x^{II} \\ \check{u}_y^{II} \end{pmatrix} \right\}. \tag{10}$$

We then define the extended elliptic projection operator $\Pi_X^a : \boldsymbol{V}_X^h(E) \to \mathbb{P}_X(E)$ for each element E, which is the solution of the following variational problem

$$\int_E \boldsymbol{\sigma}(\boldsymbol{q}_X) : \boldsymbol{\varepsilon}(\Pi_X^a \boldsymbol{v}_X^h)\, d\boldsymbol{x} = \int_E \boldsymbol{\sigma}(\boldsymbol{q}_X) : \boldsymbol{\varepsilon}(\boldsymbol{v}_X^h)\, d\boldsymbol{x} \quad \forall \boldsymbol{q}_X \in \mathbb{P}_X(E), \tag{11a}$$

with the additional conditions

$$\overline{\Pi_X^a \boldsymbol{v}_X^h} = \overline{\boldsymbol{v}_X^h}, \tag{11b}$$

$$\overline{(\Pi_X^a \boldsymbol{v}_X^h)}_R = \overline{(\boldsymbol{v}_X^h)}_R, \tag{11c}$$

where $\overline{(\cdot)}$ and $\overline{(\cdot)}_R$ represent the average translation and rotation. Then, the local extended bilinear form can be computed as:

$$\begin{aligned} a_X^{h,E}(\boldsymbol{v}_X^h, \boldsymbol{w}_X^h) &\equiv a^E\Big(\Pi_X^a(\boldsymbol{v}_X^h),\, \Pi_X^a(\boldsymbol{w}_X^h)\Big) + S_X^E\Big(\boldsymbol{v}_X^h - \Pi_X^a(\boldsymbol{v}_X^h),\, \boldsymbol{w}_X^h - \Pi_X^a(\boldsymbol{w}_X^h)\Big) \\ &= \int_E \boldsymbol{\sigma}\big(\Pi_X^a(\boldsymbol{v}_X^h)\big) : \boldsymbol{\varepsilon}\big(\Pi_X^a(\boldsymbol{w}_X^h)\big)\, d\boldsymbol{x} + S_X^E\Big(\boldsymbol{v}_X^h - \Pi_X^a(\boldsymbol{v}_X^h),\, \boldsymbol{w}_X^h - \Pi_X^a(\boldsymbol{w}_X^h)\Big), \end{aligned} \tag{12}$$

where $S_X^E(\cdot,\cdot)$ is a suitable stabilization term needed to guarantee linear consistency and stability of the method. According to the virtual element methodology, $S_X^E(\cdot,\cdot)$ can be any symmetric, positive definite, continuous bilinear form defined on the kernel of the extended projection operator Π_X^a [10]. In [17], we provide two possible choices of the stabilization term by considering the standard *dofi-dofi* and *D-recipe* formulations in our extended setting. Such choices are widely accepted in the VEM literature and in some cases they were theoretically proved to be effective to guarantee stability.

3.2 Discontinuous fields

The extended virtual element formulations presented in the previous Section can also be endowed with a structure that allows the inclusion of discontinuous fields within the virtual

element space. Let us consider a crack γ that intersects some of the elements and consider a cut element E partitioned by γ into two subdomains E^- and E^+. In order to represent two independent linear polynomials on E^- and E^+, we adopt the approach of Hansbo and Hansbo [18] and tailor it to the X-VEM. To this aim, let $N_{\text{dofs}}^{\text{VE}}$ denote the number of degrees of freedom for element E, such that $N_{\text{dofs}}^{\text{VE}} = 2N_E$ for the standard virtual element formulation and $N_{\text{dofs}}^{\text{VE}} = 4N_E$ for the extended virtual element formulation. Each one of the $N_{\text{dofs}}^{\text{VE}}$ virtual shape functions, $\boldsymbol{\varphi}_i$ on E, can be written as the sum of two new virtual shape functions $\boldsymbol{\varphi}_i^-$ and $\boldsymbol{\varphi}_i^+$ defined as follows:

$$\boldsymbol{\varphi}_i^+ = \begin{cases} 0 & \text{in } E^- \\ \boldsymbol{\varphi}_i & \text{in } E^+ \end{cases}, \quad \boldsymbol{\varphi}_i^- = \begin{cases} \boldsymbol{\varphi}_i & \text{in } E^- \\ 0 & \text{in } E^+ \end{cases}. \tag{13}$$

Repeating this procedure for all the degrees of freedom in the element, we can generate $N_{\text{dofs}}^{\text{HH}} = 2N_{\text{dofs}}^{\text{VE}}$ new discontinuous basis functions, starting from the initial $N_{\text{dofs}}^{\text{VE}}$ virtual basis functions. To define the local virtual element space to which the discontinuous approximate solution belongs, consider the following spaces:

$$\begin{aligned} \boldsymbol{V}^{h,-}(E) \equiv \Big\{ \boldsymbol{v}^h \in \big[H^1(E-)\big]^2 \,:\, \Delta \boldsymbol{v}^h{}_{|E^-} = \boldsymbol{0},\ \boldsymbol{v}^h{}_{|\partial E^-} \in [C^0(\partial E^-)]^2, \\ \boldsymbol{v}^h{}_{|e} \in \big[\mathbb{P}^1(e)\big]^2 \ \forall e \in (\partial E \cap \partial E^-),\ \boldsymbol{v}^h{}_{|E^+} = \boldsymbol{0} \Big\}, \end{aligned}$$

$$\begin{aligned} \boldsymbol{V}^{h,+}(E) \equiv \Big\{ \boldsymbol{v}^h \in \big[H^1(E^+)\big]^2 \,:\, \Delta \boldsymbol{v}^h{}_{|E^+} = \boldsymbol{0},\ \boldsymbol{v}^h{}_{|\partial E^+} \in [C^0(\partial E^+)]^2, \\ \boldsymbol{v}^h{}_{|e} \in \big[\mathbb{P}^1(e)\big]^2 \ \forall e \in (\partial E \cap \partial E^+),\ \boldsymbol{v}^h{}_{|E^-} = \boldsymbol{0} \Big\}. \end{aligned}$$

Then, the local virtual element space reads:

$$\boldsymbol{V}_X^h(E) \equiv \Big\{ \boldsymbol{v}_X^h = (\boldsymbol{v}^{h,-} + \boldsymbol{v}^{h,+}) \,:\, \boldsymbol{v}^{h,-} \in \boldsymbol{V}^{h,-}(E),\, \boldsymbol{v}^{h,+} \in \boldsymbol{V}^{h,+}(E) \Big\}. \tag{14}$$

An analogous definition of the local virtual element space for elements cut by a crack can be easily provided also for the enriched formulation presented in the previous Section.

Virtual element functions along interface edges can be reconstructed by a suitable polyharmonic approximation [15]. Finally, we obtain the following representation for the virtual element approximation on the element E cut by γ:

$$\boldsymbol{v}_X^h(\boldsymbol{x}) = \sum_{i=1}^{N_{\text{dof}}^{\text{VE}}} \left[\boldsymbol{\varphi}_i^-(\boldsymbol{x}) v_i^- + \boldsymbol{\varphi}_i^+(\boldsymbol{x}) v_i^+ \right] \quad \forall \boldsymbol{x} \in E, \tag{15}$$

where v_i^- and v_i^+ are the degrees of freedom associated with $\boldsymbol{\varphi}_i^-$ and $\boldsymbol{\varphi}_i^+$, respectively.

3.3 Stress intensity factors computation

To derive stress intensity factors, given two equilibrium states denoted by superscripts (1) and (2), we need to compute the following interaction integral:

$$I^{(1,2)} = \int_\Omega F_j(x_1, x_2) \frac{\partial w}{\partial x_j} d\Omega, \tag{16}$$

where u_i is the i-th component of the displacement field

$$F_j(x_1, x_2) = \sigma_{ij}^{(1)} \frac{\partial u_i^{(2)}}{\partial x_1} + \sigma_{ij}^{(2)} \frac{\partial u_i^{(1)}}{\partial x_1} - W^{(1,2)} \delta_{1j}, \tag{17}$$

and $W^{(1,2)} = \sigma_{ij}^{(1)} \varepsilon_{ij}^{(2)} = \sigma_{ij}^{(2)} \varepsilon_{ij}^{(1)}$ is the interaction strain energy. Then, the stress intensity factors for mode I and mode II crack opening, respectively denoted by K_I and K_{II}, are computed using the relation

$$I^{(1,2)} = \frac{2}{E'} \left[K_I^{(1)} K_I^{(2)} + K_{II}^{(1)} K_{II}^{(2)} \right], \tag{18}$$

where $E' = E$ for plane stress conditions and $E' = E/(1-\nu^2)$ for plain strain conditions. To make integral (16) computable from the X-VEM solution, which is known on the boundary only, we need to apply the divergence theorem and transform the domain integral (16) into a line integral that is evaluated on the boundaries of the element:

$$I^{(1,2)} = \sum_{E \in \Omega_J} \left(\int_{\partial E} F_j(x_1, x_2) w n_j d\Gamma - \int_E \frac{\partial F_j}{\partial x_j}(x_1, x_2) w d\Omega \right). \tag{19}$$

We then use the elliptic projection of the solution in terms of displacements to compute the corresponding deformation field and the stress components. Hence, the interaction integral can be finally computed as:

$$I^{(1,2)} = \sum_{E \in \Omega_J} \int_{\partial E} \left[\sigma_{ij}(\Pi_E^a(u_i^{(1)})) \frac{\partial u_i^{(2)}}{\partial x_1} + \sigma_{ij}^{(2)} \frac{\partial \Pi_E^a(u_i^{(1)})}{\partial x_1} - \widetilde{W}^{(1,2)} \delta_{1j} \right] w n_j d\Gamma, \tag{20}$$

where $\widetilde{W}^{(1,2)} = \sigma_{ij}(\Pi_E^a(u_i^{(1)})) \varepsilon_{ij}^{(2)}$.

For the implementation details we refer the reader to [17]. It can be shown that all the needed integrations can be carried out on the element boundary so that no volume integral needs to be computed. This is one of the main advantages of the proposed approach with respect to the X-FEM.

4 NUMERICAL EXAMPLES

4.1 Patch test

We first conduct an *extended patch test*, addressing the enrichment with singular fields and a *discontinuous patch test* needed to assess the inclusion of discontinuities as described in Section 3.2.

The extended patch test ensures that the singular enrichment fields can be exactly reproduced using the X-VEM. To this aim, we consider a square elastic plate that occupies the region $(-1, 1)^2$ under plane strain conditions, with a horizontal crack of unit length that extends from $(-1, 0)$ to $(0, 0)$. Both a coarse mesh of 10×10 square elements and a coarse mesh of 64 polygonal elements are considered, where all the nodes in the domain are enriched the near-tip displacement fields are imposed on the boundary of the domain by requiring that all the enriched boundary degrees of freedom are equal to 1 and all the standard boundary degrees of freedom are equal to 0. As

a measure for the error of the numerical solution with respect to the exact solution we adopted the relative error in strain energy, which is computed as

$$E(\boldsymbol{u}^h) = \frac{|a(\tilde{\boldsymbol{u}}, \tilde{\boldsymbol{u}}) - a(\boldsymbol{u}^h, \boldsymbol{u}^h)|}{a(\boldsymbol{u}, \boldsymbol{u})}, \tag{21}$$

where $\frac{1}{2}a(\boldsymbol{u}, \boldsymbol{u}) = 1.6776885579 \times 10^{-5}$ is the strain energy of the exact solution $\boldsymbol{u}$, and $\tilde{\boldsymbol{u}}^h$ is the projection of the discrete solution $\boldsymbol{u}^h$, which is defined as:

$$\tilde{\boldsymbol{u}}^h = \sum_{E \in \mathcal{T}} \Pi_E^a \boldsymbol{u}^h. \tag{22}$$

The relative error in strain energy for the extended patch tests is of the order of 10^{-12}, clearly showing that the X-VEM delivers sound accuracy in reproducing the enrichment fields.

In addition to the extended patch test, we perform the discontinuous patch test first proposed by Dolbow and Devan [19] in finite strain elasticity to the present context of plain strain linear elasticity. The test involves solving the problem of a 2D elastic domain occupying the unit square domain $\Omega = (0, 1)^2$ that is bisected by an horizontal crack γ into two open subdomains $\Omega^- = (0, 1) \times (0, 1/2)$ and $\Omega^+ = (0, 1) \times (1/2, 1)$. The crack is implicitly included in the model following the construction proposed in Section 3.2. As boundary conditions, we prescribe zero displacements along the edge $x = 0$, a discontinuous distribution of constant horizontal tractions along the edge $x = 1$ and zero tractions along the horizontal edges $y = 0$ and $y = 1$. For this problem, the exact solution is piecewise linear and turns out to belong to the discrete space. Indeed, as expected, the extended virtual element formulation presented in Section 3.2, passes the proposed patch test with a relative error in strain energy of 2×10^{-13}.

4.2 Convergence study

We investigate the convergence of the X-VEM for the problem of a two-dimensional square plate under plain strain conditions in the presence of a horizontal crack, extending from the boundary to the center of the specimen. The geometry of the domain is the same adopted as that for the extended patch test. On the boundary of the domain, we apply the exact near-tip mixed mode I and mode II displacement fields, which are also employed as enrichment fields for the X-VEM and represent the exact solution for the problem at hand. Both quadrilateral and general polygonal meshes are considered. To compute the element stiffness matrix, we follow two different strategies: *topological* enrichment and *geometric* enrichment. In the topological enrichment, we only enrich the node located at the singularity of the solution whereas in geometric enrichment we enrich all the nodes within a given radius from the origin. As in extended finite element methods, due to the presence of the singularity in the crack tip, the theoretical convergence rate for this problem is $R = 1$ that is non-optimal. Figure 1 shows convergence plots of the relative error in strain energy. Both VEM and X-VEM with topological enrichment converge in strain energy with a rate close to 1, in agreement with theory. It turns out that the X-VEM is insensitive to the type of mesh (quadrilaterals or polygons), and the results from the X-VEM are consistently more accurate than those from standard VEM.

Many prior studies have indicated that geometric enrichment, allows the standard X-FEM for fracture problems to recover the optimal convergence rate [20]. In order to establish if the

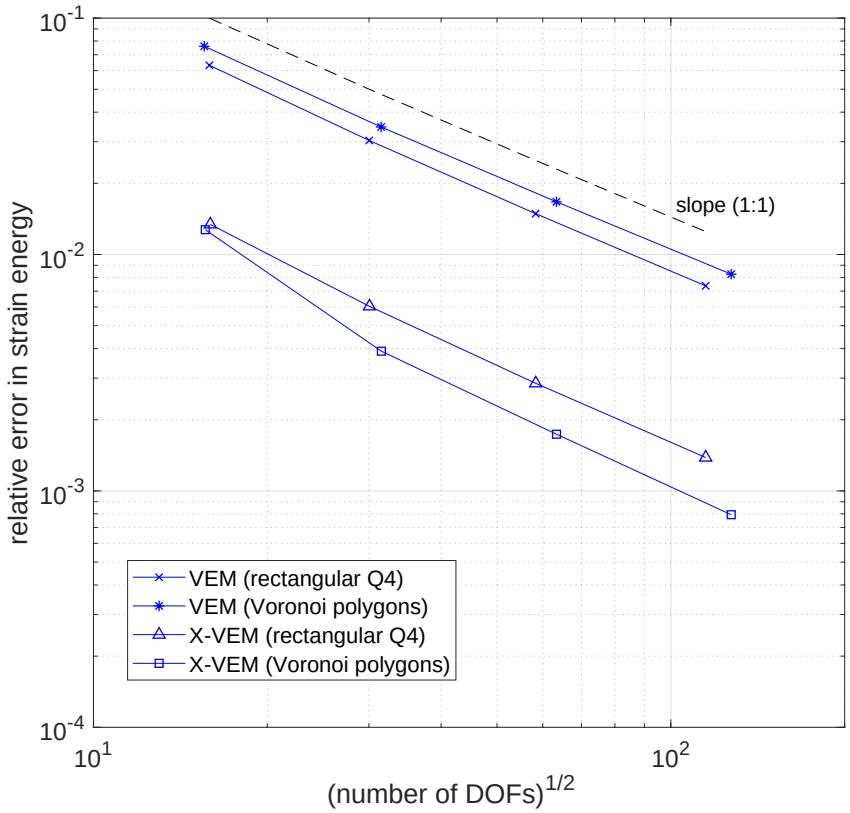

Figure 1: Convergence in strain energy for the mixed-mode benchmark problem. For the X-VEM, only the node at the origin is enriched (topological enrichment). Comparisons are shown with the standard VEM on quadrilateral and polygonal meshes. All methods converge with a rate close to unity.

proposed X-VEM can deliver the optimal convergence rate $R = 2$ that is predicted by theory, we enrich all nodes that are located within a ball of radius $r_e = 0.5$ from the origin. Figure 2 depicts convergence plots for the relative error in strain energy on quadrilateral and polygonal meshes for the X-VEM with geometric enrichment. The convergence rate is close to 2, which is consistent with theory.

5 CONCLUSIONS

- The extended virtual element method for two-dimensional elastic fracture problems, proposed in [17], allows the incorporation of crack-tip singularities and discontinuities in the approximation space.
- In the X-VEM, we augmented the standard virtual element space by means of additional vectorial basis functions that were constructed using the asymptotic mode I and mode II crack-tip displacement fields as enrichment functions.
- An extended elliptic projector was proposed that projects the functions of the extended

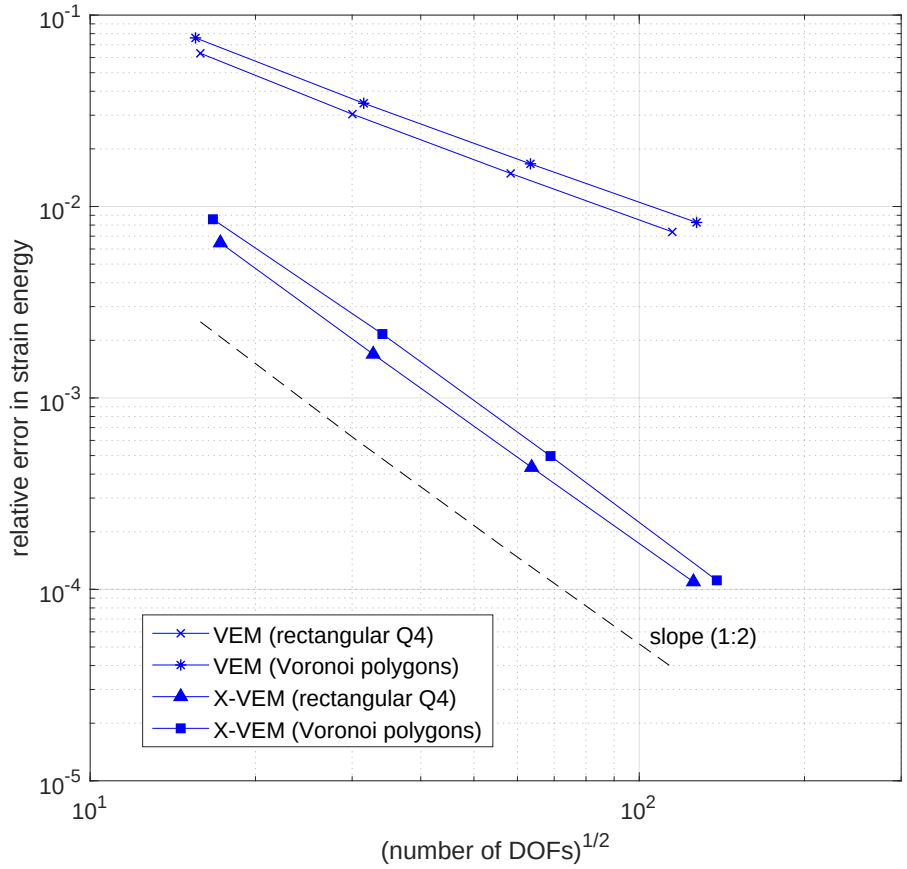

Figure 2: Convergence in strain energy for the mixed-mode benchmark problem. For the X-VEM, geometric enrichment ($r_e = 0.5$) on quadrilateral and polygonal meshes is used. Comparisons are made with the standard VEM. X-VEM converges with a rate close to two.

virtual element space onto the space spanned by linear polynomials and the enrichment fields.

- Crack discontinuities were modeled by decomposing each virtual shape function as the sum of two discontinuous shape functions, following the approach proposed by Hansbo and Hansbo [18].
- The proposed extended virtual element formulation does not present integration issues, since all integrals are computed on the elements boundary, where virtual shape functions are known.
- Many numerical tests proved the consistency and the robustness of the X-VEM.

REFERENCES

[1] J. M. Melenk and I. Babuška. The partition of unity finite element method: Basic theory and applications. *Computer Methods in Applied Mechanics and Engineering*, 139:289–314, 1996.

[2] I. Babuška and J. M. Melenk. The partition of unity method. *International Journal for Numerical Methods in Engineering*, 40:727–758, 1997.

[3] N. Moës, J. Dolbow, and T. Belytschko. A finite element method for crack growth without remeshing. *International Journal for Numerical Methods in Engineering*, 46(1):131–150, 1999.

[4] A. Tabarraei and N. Sukumar. Extended finite element method on polygonal and quadtree meshes. *Computer Methods in Applied Mechanics and Engineering*, 197(5):425–438, 2008.

[5] A. Zamani and M. R. Eslami. Embedded interfaces by polytope FEM. *International Journal for Numerical Methods in Engineering*, 88:715–748, 2011.

[6] S. E. Mousavi and N. Sukumar. Generalized Duffy transformation for integrating vertex singularities. *Computational Mechanics*, 45(2–3):127–140, 2010.

[7] E. B. Chin, J. B. Lasserre, and N. Sukumar. Numerical integration of homogeneous functions on convex and nonconvex polygons and polyhedra. *Computational Mechanics*, 56(6):967–981, 2015.

[8] E. B. Chin, J. B. Lasserre, and N. Sukumar. Modeling crack discontinuities without element-partitioning in the extended finite element method. *International Journal for Numerical Methods in Engineering*, 86(11):1021–1048, 2017.

[9] L. Beirão da Veiga, F. Brezzi, A. Cangiani, G. Manzini, L. D. Marini, and A. Russo. Basic principles of virtual element methods. *Mathematical Models & Methods in Applied Sciences*, 23:119–214, 2013.

[10] L. Beirão da Veiga, F. Brezzi, and D. Marini. Virtual elements for linear elasticity problems. *SIAM Journal on Numerical Analysis*, 51(2):794–812, 2013.

[11] A. L. Gain, C. Talischi, and G. H. Paulino. On the virtual element method for three-dimensional linear elasticity problems on arbitrary polyhedral meshes. *Computer Methods in Applied Mechanics and Engineering*, 282:132–160, 2014.

[12] V. M. Nguyen-Thanh, X. Zhuang, H. Ngyyen-Xuan, T. Rabczuk, and P. Wriggers. A Virtual Element Method for 2D linear elastic fracture analysis. *Computer Methods in Applied Mechanics and Engineering*, 340:366–395, 2018.

[13] A. Hussein, F. Aldakheel, B. Hudobivnik, P. Wrigger, P.A. Guidault, and O. Allix. A computational framework for brittle crack-propagation based on efficient virtual element method. *Computer Methods in Applied Mechanics and Engineering*, 159:15–32, 2019.

[14] E. Artioli, S. Marfia, and E. Sacco. VEM-based tracking algorithm for cohesive/frictional 2d fracture. *Computer Methods in Applied Mechanics and Engineering*, 365:112956, 2020.

[15] E. Benvenuti, A. Chiozzi, G. Manzini, and N. Sukumar. Extended virtual element method for the Laplace problem with singularities and discontinuities. *Computer Methods in Applied Mechanics and Engineering*, 356:571–597, 2019.

[16] A. Chiozzi and E. Benvenuti. Extended virtual element method for the torsion problem of cracked prismatic beams. *Meccanica*, 55:637–648, 2020.

[17] E. Benvenuti, A. Chiozzi, G. Manzini, and N. Sukumar. Extended virtual element method for two-dimensional linear elastic fracture. *Computer Methods in Applied Mechanics and Engineering*, 390:114352, 2022.

[18] A. Hansbo and P. Hansbo. A finite element method for the simulation of strong and weak discontinuities in solid mechanics. *Computer Methods in Applied Mechanics and Engineering*, 193(33-35):3523–3540, 2004.

[19] J. E. Dolbow and A. Devan. Enrichment of enhanced assumed strain approximations for representing strong discontinuities: addressing volumetric incompressibility and the discontinuous patch test. *International Journal for Numerical Methods in Engineering*, 59(1):47–67, 2004.

[20] P. Laborde, J. Pommier, Y. Renard, and M. Salaün. High-order extended finite element method for cracked domains. *International Journal for Numerical Methods in Engineering*, 64(3):354–381, 2005.